nature microbiology

Article

https://doi.org/10.1038/s41564-026-02274-x

Drought drives elevated antibiotic resistance across soils

Received: 30 July 2025

Accepted: 20 January 2026

Published online: 23 March 2026

Check for updates

Xiaoyu Shan[1], Karen Cao[2], Hannah Jeckel[1], Reinaldo E. Alcalde[1], Inês B. Trindade[1], Jarek V. Kwiecinski[3] & Dianne K. Newman[1,3]

Antibiotic resistance is a growing threat to human health and is often attributed to excessive clinical usage that selects for resistance. Although many antibiotics are derived from soil microorganisms, how environmental changes to soil ecosystems might promote resistance is poorly understood. Here we establish drought as a driving force of antibiotic resistance in the soil, with potentially far-reaching public health consequences. Across various geographic regions and soil types, we consistently observe metagenomic signatures of enrichment for antibiotic producers under drought conditions. Experimentally, we demonstrate that drought-induced lowering of water content concentrates natural antibiotics, thereby intensifying selection against sensitive strains and favouring antibiotic-resistant bacteria. Using clinical surveillance data from 116 countries, we show that the average frequency of hospital antibiotic resistance is strongly correlated with the local aridity index, even after controlling for regional income differences. Together, our findings reveal an underrecognized link between climate factors and antibiotic resistance.

Antibiotics have saved millions of lives that would otherwise have been lost to bacterial infections. Yet, their effectiveness is increasingly threatened by the rise of antibiotic resistance. Mounting clinical failures over the past decades have been largely attributed to the widespread usage—and at times, over usage—of antibiotics, which impose strong selective pressures on microbial populations[1]. Although previous research has primarily focused on the use of clinical antibiotics and its role in the evolution of resistance[1,2], a fundamental question has been overlooked: Might changes to the natural ecological source of clinical antibiotics also be relevant in promoting resistance?

Antibiotics were first discovered in experiments involving soil microorganisms as early as the 1940s, where natural products made by one soil organism were found to inhibit the growth of another[3]. Although many of these natural products have since been modified and developed into the drugs that are prescribed today, soil remains a rich reservoir of natural antibiotics that continues to be mined for drug discovery[4–6]. To survive in the presence of natural antibiotics, both antibiotic producers and non-producers alike have evolved means to withstand these compounds[7–9]. It stands to reason that many of the same mechanisms that promote tolerance or resistance to natural antibiotics confer collateral resilience to synthetically derived antibiotics that are used in human medicine[10]. Accordingly, we reasoned that if environmental conditions modulate the selective pressure arising from natural antibiotics in soil, then shifts in resistance levels amongst soil microbial communities might follow, with potential consequences for human health.

To test this hypothesis, we focused on drought as a key variable. Not only is drought a climatic stressor projected to become more frequent, severe and prolonged in the future[11], it also reduces soil water content, potentially concentrating secreted secondary metabolites—including natural antibiotics—in the soil matrix. Such concentration would be expected to intensify the selective pressure exerted by these compounds, leading to enrichment of both antibiotic producers and resistant taxa. Several observations are consistent with this prediction. For example, higher frequencies of bacteria producing phenazine antibiotics have been reported in drier rhizosphere soils[12,13]; another

[1]Division of Biology and Biological Engineering, California Institute of Technology, Pasadena, CA, USA. [2]Division of Engineering and Applied Science, California Institute of Technology, Pasadena, CA, USA. [3]Division of Geological and Planetary Sciences, California Institute of Technology, Pasadena, CA, USA. e-mail: dkn@caltech.edu

https://doi.org/10.1038/s41564-026-02274-x

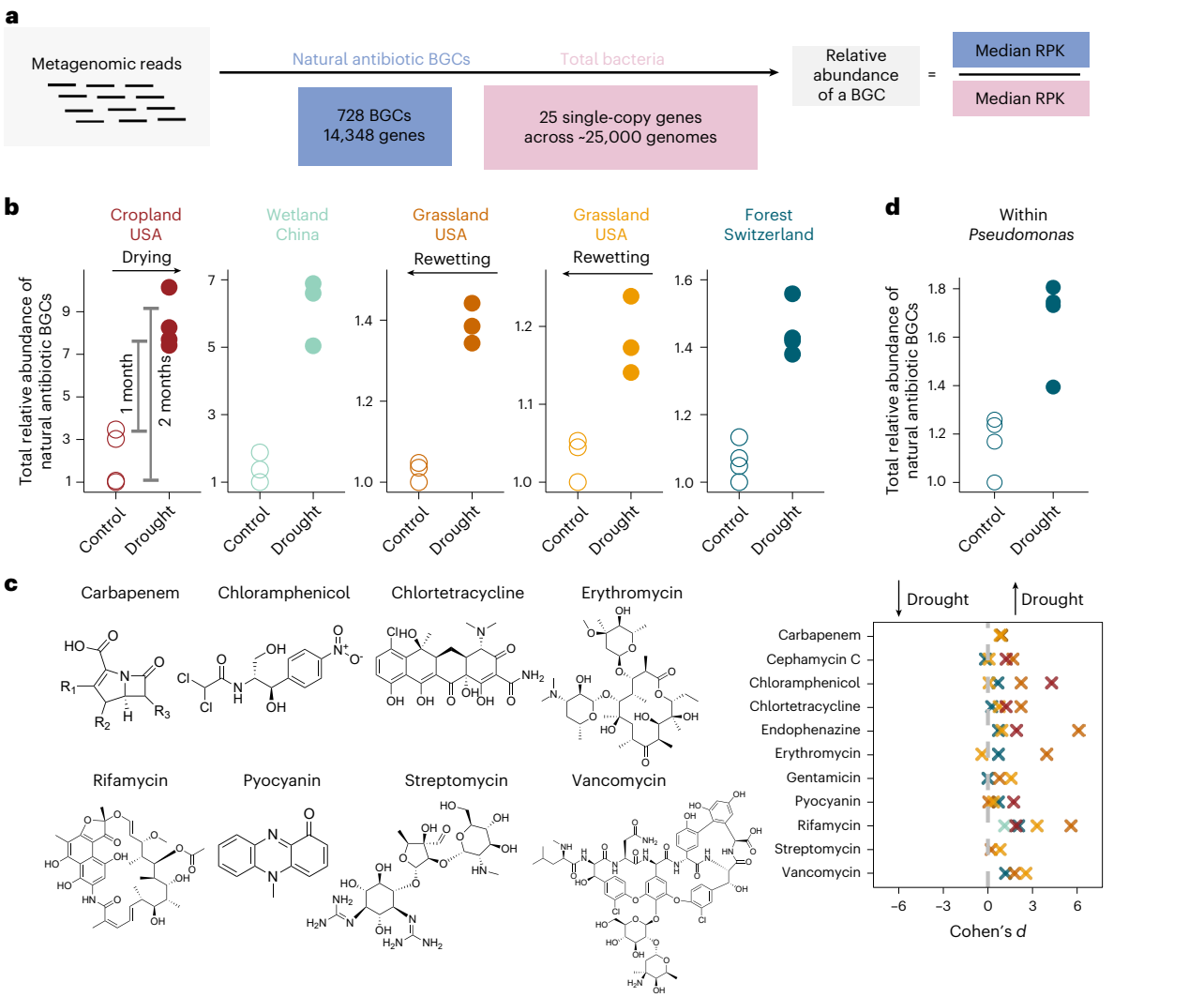

Fig. 1 | Significant enrichment of antibiotic biosynthesis genes under drought conditions in soil. a, A schematic illustration of the computational pipeline[27]. **b**, Total relative abundance of natural antibiotic BGCs under drought and control conditions, normalized by the minimum value within each dataset to facilitate cross-dataset comparisons. RPK refers to the mapped reads per kilobase length of the reference gene. The number of biological replicates used in each dataset is 4, 3, 3, 3 and 4. **c**, Representative structures of natural antibiotics whose biosynthesis genes found to be enriched under drought conditions. Positive values of Cohen's *d* indicate enrichment under drought, that is, $d = 3$ indicates 3 standard deviations higher in drought conditions[72]. **d**, Antibiotic BGCs were also significantly enriched under drought conditions within the *Pseudomonas* population. The data shown are from the Swiss forest dataset; results for the other datasets are presented in Extended Data Fig. 3.

study found greater richness of nonribosomal peptide adenylation and polyketide ketosynthase domain fragments—markers of secondary metabolite biosynthesis—in arid soils[14]. Higher abundance of several antibiotic compounds such as streptamine sulfate has also been found in dryer soils[15].

Building on these observations, we set out to determine whether and how drought shapes antibiotic biosynthesis and resistance in global soils via a combination of computational and experimental approaches. We further analysed global hospital isolates data to highlight potential public health consequences of drought-driven elevation of antibiotic resistance in soil ecosystems.

Results

Drought enriches antibiotic biosynthesis genes in soils

Using a culture-independent approach, we began to assess whether drought influences antibiotic biosynthesis in soil by compiling five metagenomic datasets. Within each dataset, drought and control conditions were the only variables in the experimental design[16–19] (Methods). This selection criterion was applied to minimize confounding effects, which are common in large-scale ecological studies—for example, covarying temperature in seasonal samples or site-specific differences of soil properties in latitudinal/longitudinal comparisons. The selected datasets span geographically distinct regions (USA, China and Europe) and encompass diverse land use types, including cropland, grassland, forest and wetland—together providing a comprehensive, global-scale perspective. We developed a standardized pipeline (Fig. 1a) to compare the abundance of antibiotic biosynthesis genes between treatments by incorporating a curated set of 728 biosynthetic gene clusters (BGCs), encoding natural products with documented antibacterial activity[20]. To account for differences in sequencing depth, we normalized BGC abundance against 25 universally single-copy housekeeping genes present across bacterial genomes[21] (Methods).

Strikingly, in all five datasets, the relative abundance of antibiotic biosynthesis genes was significantly higher under drought conditions ($P < 0.008$; Fig. 1b and Supplementary Table 1). This trend is true for both wet-to-dry shifts (that is, increasing abundance after

drying, cropland metagenomes in Fig. 1b) and dry-to-wet shifts (that is, decreasing abundance after rewetting, grassland metagenomes in Fig. 1b). Within the same dataset, the enrichment becomes stronger when the duration of drought is longer (for example, 1 versus 2 months; Fig. 1b, first panel). Such enrichment is not observed for all genes; as a negative control, we quantified the relative abundance of the bacterial chemotaxis gene *cheA*, finding its relative abundance does not change significantly or even decreases under drought (Extended Data Fig. 1). In addition, genes that are expected to be neutral to drought do not show significant differences between drought and control conditions ($P \approx 0.07–0.91$; Extended Data Fig. 1 and Supplementary Table 1). The observed enrichment of antibiotic biosynthesis genes under drought spanned multiple antibiotic classes, including β-lactams (for example, carbapenem and cephamycin), phenazines (for example, pyocyanin and endophenazine), macrolides (for example, erythromycin) and aminoglycosides (for example, gentamicin and streptomycin), as illustrated in Fig. 1c. Many of these compounds are not only produced by soil bacteria but also play important roles in modern clinical treatments.

To understand the factors driving this enrichment, we considered the possibility that drought preferentially favours monoderm Gram-positive bacteria[22,23]—particularly *Streptomyces*, a genus well known for its prolific antibiotic production. Indeed, *Streptomyces* accounted for 63.8% of the antibiotic biosynthesis genes identified across the datasets we analysed (Extended Data Fig. 2). To disentangle antibiotic biosynthesis from potential confounding effects of monoderm enrichment during drought, we repeated our analysis using only sequences derived from *Pseudomonas*, a Gram-negative genus not typically favoured under drought[22,23] but capable of producing natural antibiotics. Even within the *Pseudomonas* population, the enrichment of biosynthetic genes under drought conditions largely remained significant ($P < 0.02$ for four datasets and $P = 0.08$ for the US cropland dataset; Fig. 1d and Extended Data Fig. 3). This finding aligns with prior culture-dependent studies reporting that phenazine-producing *Pseudomonas* are more prevalent in dryer rhizosphere soils[12,13]. Moreover, a recent study profiling redox-active metabolites—many of which are natural antibiotics—across a large number of bacterial isolates suggested these metabolites are more prevalent in dryer soils, including those produced by diverse members of the Proteobacteria[24]. Taken together, these results suggest that antibiotic biosynthesis itself is a beneficial trait under drought stress and that its selection is not solely tied to community shifts reflecting selection for monoderm cell wall architecture. Although the structural resilience of *Streptomyces* can contribute to its success under drought, the ability to produce—and thus resist—antibiotics may itself be an important factor enhancing fitness under drought conditions.

Drying concentrates antibiotics and intensifies selection

To understand the mechanism of antibiotic-producing bacteria enrichment under drought, we developed an experimental method using soil microcosms to test our hypothesis that drought intensifies selection for antibiotic-producing microorganisms by concentrating antibiotics within the soil matrix (Methods). Although it is possible that drought might upregulate the production of certain antibiotics, resulting in their enrichment, we found an insignificant increase of relative expression level (metatranscriptomic reads per kilobase/metagenomic reads per kilobase) for antibiotic biosynthesis genes on a community level[25] ($P = 0.69$; Extended Data Fig. 4). Rather, we predicted that the increased concentration of antibiotics due to decrease in soil water content upon desiccation would amplify selection against susceptible community members while favouring resistant or antibiotic-producing strains (Fig. 2a). In our experimental microcosms, synthetic soils initially free of bacteria and antibiotics were inoculated with soil bacteria isolated from Washington State University's Lind Dryland Research Station[26] and supplemented with a known antibiotic, permitting a well-controlled experimental setup. Starting from identical baseline conditions, we mimicked drought and control conditions by adjusting evaporation rates (Methods). Differential evaporation rates gradually led to distinct soil water content over a 3-day period, resulting in a threefold increase in effective bulk antibiotic concentration (Fig. 2b). We selected a 3-day drying window to mimic a short-term drought exposure, consistent with the timescale at which significant metagenomic changes were observed in natural grassland soils (Fig. 1b). The same concentrating effect can be expected under longer drought durations.

Using phenazine-1-carboxylic acid (PCA) as a representative natural antibiotic, we assessed its selective potency under drying treatment. PCA represents a broad family of phenazine compounds that are widely distributed in global soils[27] and are known to confer collateral resistance to clinical antibiotics[28,29]. PCA can kill sensitive bacteria by inducing oxidative stress, while bacteria can tolerate and resist PCA if they possess certain efflux pumps and oxidative stress response enzymes[26]. Using our soil microcosm system, we tested multiple soil bacterial species from our dryland isolate collection with respect to PCA tolerance[26]. Their relative fitness was measured by the number of colony-forming units (CFUs) following PCA treatment normalized by CFUs without PCA exposure, measured under either drying or control conditions. We set the initial PCA concentration to 100 μM based on its environmental relevance[26]; this concentration diverged over time between drying and control conditions due to differential water loss. We found that PCA-sensitive strains such as *Chryseobacterium shigense* (Bacteroidetes) exhibited over 99% reduction in relative fitness under drying conditions but only around 5% reduction under control conditions ($P = 0.01$ between drying and control; Fig. 2c), a pattern comparable to that observed by directly increasing PCA concentration threefold under control conditions (Fig. 2d). By contrast, PCA-resistant species such as *Pseudomonas synxantha* (Pseudomonadaceae) showed no significant difference in relative fitness between drought and control conditions ($P = 0.61$; Fig. 2c). This pattern held true across other phylogenetic clades—for example, *Arthrobacter pascens* (Actinobacteria, PCA-sensitive, $P = 0.003$) versus *Pantoea agglomerans* (Enterobacteriaceae, PCA-resistant, $P = 0.86$)—demonstrating that drying-induced antibiotic concentration selectively disadvantages susceptible taxa while enriching for tolerant ones, including producers who are intrinsically resistant to the antibiotics they synthesize.

If concentration indeed drives the enrichment of antibiotic tolerant bacteria, we reasoned that we should be able to observe similar enrichment for other traits in the metagenomic datasets that would be subject to positive selection due to concentration. To test this hypothesis, we searched for genes encoding the type VI secretion system (T6SS)—a contact-dependent mechanism often used by bacteria to kill neighbouring cells[30]. Under drought, as bacterial cells become more physically concentrated within reduced pore spaces, traits such as T6SS should also confer a greater competitive advantage[31]. Because T6SS have been described primarily in Gram-negative bacteria such as *Vibrio* and *Pseudomonas*—the former being more relevant to marine environments—we focused our analysis on *Pseudomonas* populations within our soil datasets. As predicted, we observed a significant increase in the relative abundance of T6SS effector genes under drought across all five metagenomic datasets ($P < 0.03$; Extended Data Fig. 5). These findings reinforce the conclusion that drought-driven concentration effects intensify selection and contribute to functional shifts in soil microbial communities.

Elevated antibiotic resistance in soils under drought

Having experimentally demonstrated that drying-induced concentration of natural antibiotics favours antibiotic-resistant bacteria over susceptible ones, we predicted that the relative abundance of antibiotic resistance genes should also increase under drought. To test this prediction, we reanalysed the same five soil metagenomic datasets used in our analysis of antibiotic biosynthesis, finding that the relative abundance of antibiotic resistance genes was significantly higher under

https://doi.org/10.1038/s41564-026-02274-x

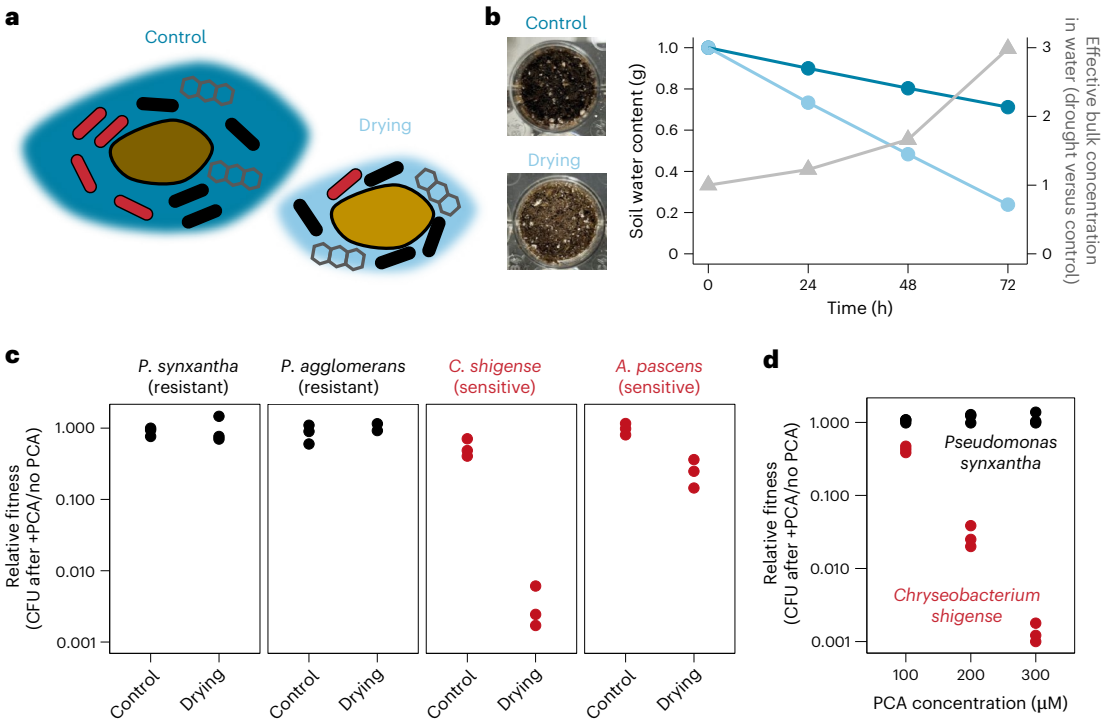

Fig. 2 | Drying intensifies selection by concentrating antibiotics. a, A schematic illustration of drought-induced concentration of natural antibiotics. Soil bacteria (red and black rods) and natural antibiotic molecules (grey tri-hexagons) are depicted within a water layer (blue) surrounding a soil particle (tan oval). Drying reduces water content, thereby concentrating antibiotics, which selectively disadvantages sensitive (red) bacteria relative to resistant (black) bacteria. **b**, Left: synthetic soil microcosms subjected to drying and control treatments for 3 days inoculated with bacteria known to be either sensitive or resistant to PCA. Photographs were taken at the end of the incubation period. Right: water content in each condition. The average of measurements for two replicates are shown. Dark blue: control conditions; light blue: drying conditions. The grey line indicates relative bulk concentration of phenazine in water under drying conditions compared with under control conditions, calculated based on initial concentrations. The error bar indicating standard error is smaller than the size of the symbols. **c**, Relative fitness of sensitive and resistant strains (defined as CFUs in soil with 100 uM PCA normalized by CFUs without PCA, either under drying or control conditions) in soil microcosms after 3 days. **d**, Relative fitness of sensitive and tolerant bacteria under control conditions following exposure to a range of initial PCA concentrations.

drought in all cases ($P < 0.008$; Fig. 3a). This observation is consistent with previous findings reporting increased antibiotic resistance gene abundance in estuarine sediments during drier spring seasons compared to wetter summer months[32]. Moreover, antibiotic resistance gene abundance was strongly correlated with the abundance of antibiotic biosynthesis genes (Pearson's $r > 0.80$, $P < 0.01$), supporting the idea that elevated resistance reflects increased selective pressure from natural antibiotics. Taxonomic composition analysis of antibiotic resistance genes suggests that resistance is not limited to antibiotic producers themselves but also accumulates in non-producing taxa subject to antibiotic-driven selection (Extended Data Fig. 2). For example, *Rhodococcus* and *Nocardia*, which only accounted for <1% of increase in antibiotic biosynthesis genes, both contributed >20% of the increase in antibiotic resistance genes. *Streptomyces*, while contributing 63.8% of antibiotic biosynthesis genes in our datasets, accounted for only 14.6% of antibiotic resistance genes detected.

In addition to finding metagenomic evidence indicating that drought selects for antibiotic resistance, we also tested whether such a relationship could be validated phenotypically. We collected natural soil samples from the California Institute of Technology (Caltech) campus containing intact microbial communities and their endogenous antibiotic compounds (Extended Data Fig. 6). As with the synthetic soil microcosms, each sample underwent drying treatment to mimic the drought process and was compared with control conditions (Fig. 3b). After 3 days of incubation, we quantified the resistance frequency of members of the microbial communities in each treatment, defined as the number of CFUs that grew on a selective medium containing antibiotics, normalized by the number of CFUs that grew on the same medium without antibiotics (Fig. 3b). We tested four molecules representing different antibiotic classes: ampicillin (a β-lactam targeting cell wall biosynthesis), ciprofloxacin (a fluoroquinolone targeting DNA replication), kanamycin (an aminoglycoside targeting protein synthesis) and PCA (a phenazine generating reactive oxygen species). Consistent with the metagenomic data, we found that soils exposed to drying treatment exhibited significantly higher resistance phenotypes than controls overall (paired Wilcoxon test, $P = 5.3 \times 10^{-6}$; Fig. 3c), confirming that drought selects for antibiotic resistance.

Global correlation between clinical resistance and aridity

The enrichment of antibiotic-resistant genes and antibiotic-resistant bacteria in drought-stressed soils may have important implications for human health. Many of the taxa enriched under drought—such as *Nocardia*, *Streptomyces* and *Mycobacterium* (Extended Data Fig. 2)—have close relatives that are known human pathogens, including *Nocardia asteroides*[33], *Streptomyces somaliensis*[34], *Mycobacterium tuberculosis*[35] and *Mycobacterium leprae*[36]. Furthermore, antibiotic-resistant genes can be transferred from environmental microorganisms to human pathogens via horizontal gene transfer (HGT), even across long phylogenetic distances. Prior studies have found evidence for recent antibiotic-resistant gene exchange between soil bacteria and clinical pathogens[37], including from natural antibiotic producers[38]. Furthermore, the rate of HGT is also expected to be higher in dryer soils[31]. Consistent with these findings, we also observed that some drought-enriched antibiotic resistance genes in soil showed signs of

https://doi.org/10.1038/s41564-026-02274-x

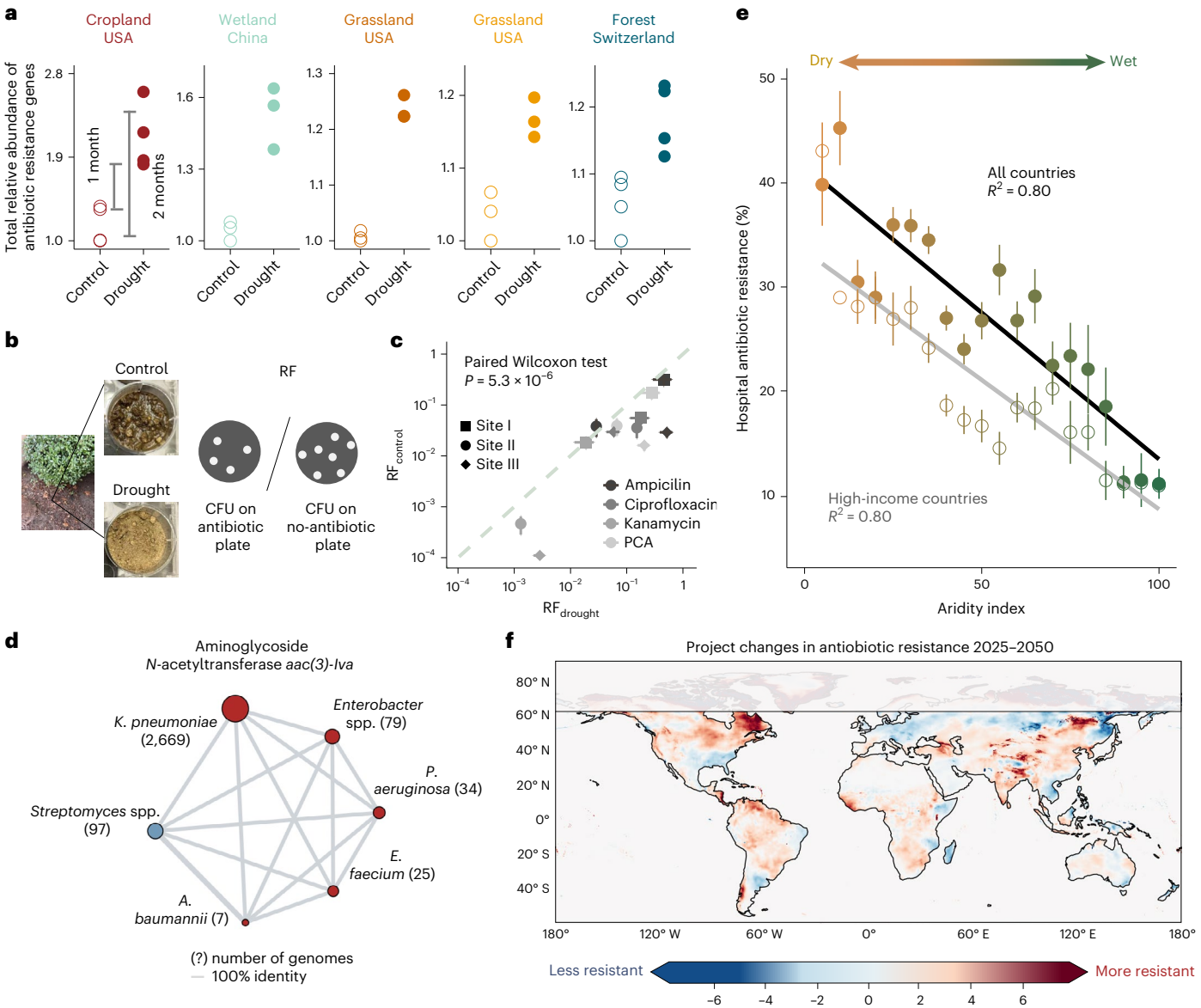

Fig. 3 | Genotypic and phenotypic evidence for elevated antibiotic resistance under drought. a, Relative abundance of antibiotic resistance genes under drought and control conditions, normalized by the minimum value within each dataset for cross-dataset comparison. Number of biological replicates used in each dataset is 4, 3, 3, 3 and 4. **b**, Experimental setup using natural soil microcosms to quantify phenotypic antibiotic resistance. **c**, Phenotypic resistance frequency (RF) is significantly higher under drying conditions compared with controls (falling in the region below the line of equivalency). The data are presented as mean values ± standard error calculated from two technical replicates. The *P* value is generated from one-sided paired Wilcoxon test. **d**, Recent HGT of drought-enriched antibiotic resistance genes across ESKAPE pathogens (red nodes). The blue node indicates non-ESKAPE pathogen taxon often found in soil. The edges represent 100% sequence identity. The values in brackets indicate the number of genomes harbouring 100% identical sequences. Network structure was visualized by R package visNetwork. **e**, Strong positive correlation between the De Martonne aridity index and the average frequency of antibiotic resistance among clinical isolates across more than 100 countries. The closed dots and black line indicate all countries, whereas open dots and grey lines indicate high-income countries (per capita gross national income >US$13,846 per World Bank definition). The data are presented as mean values ± standard error. Resistance frequencies were averaged within consecutive intervals of aridity index to visualize the trend; see Extended Data Fig. 8 for full dataset. **f**, Predicted changes in average hospital antibiotic resistance frequency—as in **c**—from 2025 to 2050, based on climate model projections of De Martonne aridity index shifts, excluding latitudes greater than 60° N covered by permafrost[48]. The prediction was made based on the SSP2-4.5 moderate scenario and depicts the average of projections based on three widely used climate models GISS-E2-1-G, MPI-ESM1-2-HR and HadGEM3-GC31-LL. RF, resistance frequency.

recent HGT across pathogens. For example, *aac(3)-Iva*, an aminoglycoside *N*-acetyltransferase conferring resistance to aminoglycosides, was enriched under drought (median Cohen's $d = 0.70$). A bioinformatic search of public databases revealed that this gene is present in common soil taxa such as *Streptomyces* (97 genomes) and *Rhodococcus* (2 genomes), as well as in a large number of clinical ESKAPE pathogen (a group of highly virulent bacteria that often "escape" the effects of common antibiotics) genomes, including *Enterococcus faecium* (25 genomes), *Klebsiella pneumoniae* (2,669 genomes), *Acinetobacter baumannii* (7 genomes), *Pseudomonas aeruginosa* (34 genomes) and *Enterobacter* spp. (79 genomes) (genomes accessions were detailed in NCBI Identical Protein Groups ID: WP_001199192.1; Fig. 3d). Strikingly, all of these soil and clinical genomes share this antibiotic-resistant gene with 100% sequence identity, indicating recent or even ongoing horizontal transfer. Similarly, *acc-4*, a class C β-lactamase hydrolysing cephalosporin that was enriched in soil under drought

(median Cohen's d = 0.81), also shows signs of recent HGT between *A. baumannii* and *K. pneumoniae* (detailed in NCBI Identical Protein Groups ID: WP_063857708.1; Extended Data Fig. 7). These findings point to recent gene flow between soil and clinical bacteria and suggest that drought-enhanced resistance in environmental reservoirs may have direct implications for the spread of antibiotic resistance in clinical pathogens.

Previous studies have further shown frequent transmission of bacteria from soil to humans through various pathways such as agriculture[39], recreation[40] and dust inhalation[41], motivating us to ask whether drought leaves a detectable signature in the frequency of clinical antibiotic resistance. To test this hypothesis, we analysed antibiotic resistance data from hospitals collected in over 100 countries, along with climate data corresponding to each hospital's geographic location[42]. Using annual precipitation (P) and mean temperature (T), we calculated the De Martonne aridity index[43], defined as $P/(T+10)$, to approximate the cumulative effects of drought at each site. Remarkably, we found a strong negative correlation between aridity index and the average frequency of resistant clinical isolates (R^2 = 0.80; Fig. 3e and Extended Data Fig. 8), suggesting that climate-driven selection in soil ecosystems may have far-reaching consequences for global public health. To control for economic factors that might covary with aridity but independently influence resistance rates—possibly through antibiotic stewardship and healthcare infrastructure—we repeated the analysis using only high-income countries (defined as having a per capita gross national income >US$13,846, according to World Bank). The overall hospital antibiotic resistance frequency decreased by 8% in this subset (parallel downshifting of the fitting line in Fig. 3e), indicating that economic factors do contribute to hospital antibiotic resistance. However, the negative correlation between hospital antibiotic resistance and the aridity index remained equally strong (R^2 = 0.80; Fig. 3e), reinforcing the robustness of the association between climate aridity and clinical resistance, independent of country economic income level.

We further leveraged this linear relationship to predict future changes in resistance burden for regions undergoing climatic transitions in De Martonne aridity index as a function of temperature and precipitation. Specifically, we considered three Shared Socioeconomic Pathways (SSPs)[44]—SSP1-2.6 (best case) (Extended Data Fig. 9b), SSP2-4.5 (moderate) (Extended Data Fig. 9a) and SSP5-8.5 (worst case) (Extended Data Fig. 9c)—each representing a different greenhouse gas emissions scenario. For each pathway, we averaged projections from three widely used climate models: GISS-E2-1-G[45], MPI-ESM1-2-HR[46] and HadGEM3-GC31-LL[47], to estimate changes in aridity index from 2025 to 2050. Although high-latitude regions in the Northern Hemisphere are projected to undergo substantial temperature increases, we exclude them from our projection because rising temperature in these regions would be expected to lead to permafrost melting rather than an increase in soil aridity[48]. Our projections indicate that every populated continent contains regions that may face a heightened risk of antibiotic resistance emergence driven by climate change, motivating future work to monitor such changes (Fig. 3f).

Discussion

In this study, we demonstrate that drought consistently selects for elevated antibiotic resistance in soil microbial communities, at both the genotypic and phenotypic levels. Furthermore, we showed that regional aridity is strongly correlated with the prevalence of antibiotic resistance in clinical settings across more than 100 countries. These findings point to the existence of an environmental 'soil–clinic axis', which operates in parallel to the traditional drug discovery pipeline derived from soil microorganisms. Although the conventional soil–clinic axis has focused on the beneficial extraction of antibiotics from soil, our results suggest that environmental selection exerted by these ubiquitous soil natural products may contribute to the global burden of clinical resistance. Central to this concept is the recognition that natural antibiotics are structurally or functionally connected to clinically used drugs and that this similarity promotes selection for collateral antibiotic resilience[10].

We propose that a key mechanism driving resistance enrichment under drought is the concentrating effect: as soil dries, natural antibiotics—especially their bioavailable, aqueous-phase fraction—become more concentrated in the remaining pore water. Beyond this direct effect, drought also introduces additional, more nuanced mechanisms that may influence the selective strength of antibiotics. For instance, studies in pure culture have shown that osmotic stress can sometimes modulate antibiotic activity, in some cases enhancing[49,50] and in other cases reducing drug effectiveness[51,52], depending on the compound and the physiology of the organism[53]. Moreover, prolonged drought may also alter the degradation rates of certain antibiotics in soil. Studies have shown that reduced soil moisture can slow down the degradation of some antibiotics[54] but accelerate others[55]. Despite these context-specific effects, we argue that the heightened concentration of antibiotics under drought provides a direct, robust, broadly applicable and ecologically relevant mechanism. It explains the consistent enrichment of both biosynthesis and resistance genes across different classes of natural antibiotics, diverse environments and varying timescales.

The strong correlation between aridity and clinical antibiotic resistance is concerning given anticipated global climatic changes. We note that the observed correlation is based on cross-sectional data, and additional research is needed to trace the pathways of gene flow from soil to the clinic to demonstrate a causal relationship. Future studies are also needed to examine the drought–antibiotic resistance relationship across more geographically diverse soils (for example, Africa) in addition to those from previous studies. Nevertheless, our study offers a clear example of how climate change has the potential to intersect with microbial ecology to shape public health outcomes. These findings underscore the importance of integrating environmental and clinical perspectives within a unified One Health framework[56,57]. As climate instability intensifies, such integrative approaches will be critical for anticipating and mitigating the global trajectory of antibiotic resistance.

Methods

Metagenomic analysis

We compiled five metagenomic datasets from four previous studies in which drought was the only variable in the experimental design. This selection criterion was applied to minimize confounding effects, which are common in large-scale ecological studies that often rely on black-box statistical methods with varying degrees of reliability and interpretability. For instance, we excluded comparisons such as dry summer versus wet winter, where temperature also differs. Similarly, we did not use data based on latitudinal or longitudinal gradients, as such datasets involve samples from widely separated locations with highly heterogeneous soil characteristics. The final datasets selected include: (1) cropland in California, USA[16], where sorghum rhizosphere samples under no-irrigation and regular watering conditions were collected with two replicates per condition per timepoint (two timepoints (4 weeks and 8 weeks) under drought or control conditions were selected, yielding eight metagenomes into our collection); (2) grassland in California, USA[17], where near-surface soil was sampled at the end of the dry season, along with soil collected after 3 days of rewetting, with three replicates per condition (two sites (Hopland and McLaughlin) were selected into our collection, each with six metagenomes); (3) a forest site in Valais, Switzerland[18], where Scots pine forest soil was sampled either without irrigation or under doubled-precipitation, each with four replicates, yielding eight samples; and (4) a wetland in Nanchang, China[19], where natural soils with high and low water content (~6.7-fold difference) were designated as wet and drought treatments, each with three replicates, for a total of six metagenomes (National Microbiology Data Center, ID: NMDC20147401).

We developed a computational pipeline to quantify the relative abundance of antibiotic biosynthesis genes and antibiotic resistance

genes. To construct a reference for biosynthesis genes, we filtered the 3,013 BSGs from the MIBiG database[20] (version 4.0) to retain only those with documented antibacterial activity, removing retired entries, resulting in 728 BSGs. We further excluded genes annotated as transporters or transcriptional regulators to avoid ambiguous mappings, resulting in a curated set of 14,348 genes. For antibiotic resistance genes, we compiled 6,048 sequences from the CARD database (December 2024 release)[58]. To normalize for sequencing depth, we constructed a total-bacteria reference gene set based on the bac120 single-copy marker set, downloaded from the Genome Taxonomy Database[21]. We selected the 25 most ubiquitous genes and extracted their protein sequences for downstream normalization as described in our previous work[27].

Metagenomic raw reads were quality-filtered using fastp[59] (version 0.23.2) with default parameters, and then mapped to the protein database using DIAMOND[60] (version 2.1.8.162) with the -k 1 option to retain only the best hit. Translated reads mapping below 80% amino acid identity were discarded, and read counts were normalized by average gene length. For each gene in the reference set, a normalized score of reads per kilobase length was calculated and divided by the median score of the total-bacteria genes to produce a relative abundance estimate. This approach has been benchmarked in our previous work[27]. To calculate Cohen's *d* for each biosynthesis gene cluster, we quantified the median of relative abundance estimate for all genes in each biosynthesis gene cluster for each sample under drought or control conditions.

To assess biosynthesis gene abundance specifically in *Pseudomonas*, we repeated this mapping process using a curated set of 31 biosynthesis clusters together with housekeeping genes from *Pseudomonas* genomes. To quantify T6SS effector genes, we leveraged a set of 12,306 reference genes (SecReT6 version 3) of T6SS effector genes derived from *Pseudomonas* genomes[61]. To prevent artificial inflation of correlations between antibiotic biosynthesis genes and antibiotic resistance genes due to potential overlaps, we removed any biosynthesis genes showing homology to antibiotic resistance genes (>50% amino acid identity and >80% coverage) using MMseqs2[62] before calculating their correlations. We leveraged a published dataset[25] with coupled metagenomics and metatranscriptomics to evaluate the relative expression level of natural antibiotic biosynthesis genes, which is quantified by the ratio of metatranscriptomic reads per length and metagenomic reads per length mapped to the aforementioned curated set of reference genes for antibiotic biosynthesis. To identify recent HGT events of antibiotic resistance genes, we searched the NCBI database of Identical Protein Groups for gene sequences with 100% homology that are present in different species. The full list of different species carrying identical sequences *aac(3)-Iva* and *acc-4* genes are detailed under NCBI Identical Protein Groups ID WP_001199192.1 and WP_063857708.1.

All metagenomic analyses were performed on the Caltech Resnick HPC cluster. Gene sharing network was visualized by R package visNetwork[61–63].

Soil microcosm experiments

We established a controlled experimental system for soil microcosms. Soil bacteria were isolated from soil samples collected from a wheat field at Washington State University's Lind Dryland Research Station, as previously described[26]. Synthetic soil consisted of 70–80% sphagnum peat moss blended with perlite and calcium silicate (Sun Gro Horticulture Canada). The mixture was autoclaved and dried overnight at 55 °C before use. We inoculated 0.1 g of synthetic soil into each well of a 12-well plate. Each well received 1 ml of water, either containing 100 μM PCA (treatment) or no antibiotic (control). Based on the measured bulk density (8.5 ml g^{-1}), this corresponded to a volumetric water content of 54.1% (v/v). Bacterial cultures grown overnight in Luria–Bertani (LB) medium were added at 50 μl per well and mixed thoroughly using a pipette tip. To prevent cross-contamination, empty wells were placed between wells inoculated with different bacteria or conditions. Plates were incubated at 30 °C. Control groups were covered with standard plastic lids that allowed slow evaporation, while drought groups were covered with breathable paper film to accelerate evaporation. Water loss was recorded at 24, 48 and 72 h to calculate differences in water content and effective antibiotic concentration between the two treatments. After 3 days of incubation, soil from each well was transferred into 5 ml PBS in a 50 ml Falcon tube using a plastic spatula. The well was then washed with an additional 5 ml PBS to collect any remaining bacteria. Samples were vortexed for 1 min and sonicated for 1 min to release bacteria into the liquid phase. The suspension was serially diluted in a 96-well plate and spotted on LB agar plates for CFU counting.

Phenotypic quantification of antibiotic resistance

Natural soil samples were collected from three locations on the Caltech campus (Pasadena, CA, USA) (Extended Data Fig. 6). Soil was transported in 50 ml Falcon tubes, and 2 g from each site was placed in a six-well plate. Each well received 1 ml of water. Drought treatments were covered with breathable paper film, while control treatments were covered with standard plastic lids, as described above. All plates were incubated at 30 °C for 3 days. After incubation, CFUs were measured on tryptic soy broth agar with and without antibiotics. To suppress fungal growth, all plates were supplemented with 100 μg ml^{-1} cycloheximide. The antibiotics used were kanamycin (50 μg ml^{-1}), ciprofloxacin (1 μg ml^{-1}), ampicillin (100 μg ml^{-1}) and PCA (100 μM). Plates were incubated at room temperature with light shielding for 2 days. Because natural microbial communities produce colonies with variable size and growth rates, we used one agar plate per dilution rather than multi-spotting. For each condition, two technical replicates (plates) were included to reduce counting noise. CFUs were counted using a digimatic colony counter (Labline Instruments), selecting only those dilution plates with 10–200 colonies. We performed this experiment twice: on 7 February 2025 (after a rainfall event), testing kanamycin and ciprofloxacin, and again on 14 February 2025 (also after a rainfall event), testing ampicillin and PCA. In total, this experiment consumed: 3 sites × (4 antibiotics + 2 no antibiotic controls) × 4 dilutions × 2 technical replicates × 2 conditions (drought versus wet control) = 288 agar plates.

We note that this approach captures only a subset of soil microorganisms that are culturable on tryptic soy broth and form colonies within 2 days. However, because resistance frequency was calculated as the ratio of CFUs on selective versus non-selective media and compared between drought and control treatments from the same starting inoculum, variation in cultivability or growth rate was internally controlled.

Hospital data and climate projections

The hospital antibiotic resistance data and its accompanied data of annual mean temperature and annual precipitation were requested from the authors of a recent global-scale study[42]. This recent study represents a comprehensive global-scale effort to aggregate and analyse hospital antibiotic resistance frequencies, laying a critical foundation to investigate the linkage between clinical resistance and environmental factors. The data were collected from hospitals across 116 countries, where antibiotic resistance frequency was defined as the proportion of tested hospital isolates—restricted to antibiotics with ≥30 tested isolates—that were classified as non-susceptible. We calculated the De Martonne aridity index for each hospital location as $P/(T+10)$, where P is annual precipitation and T is annual mean temperature[43]. For each five-unit consecutive interval of the aridity index, we calculated and reported the average frequency of resistant clinical isolates and the associated standard error. The per capita gross national income data were accessed from the database of the World Bank[64].

We obtained daily global climate projections at 0.25° × 0.25° resolution from the NASA Earth Exchange Global Daily Downscaled Projections (NEX-GDDP-CMIP6) dataset[65,66]. The Coupled Model Intercomparison Project (CMIP) systematically compares climate

models across various organizations under shared socioeconomic pathways (SSPs), which represent different greenhouse gas emissions scenarios[44,67]. For our analysis, we selected three climate models: GISS-E2-1-G from NASA's Goddard Institute for Space Studies[45] and two additional high-performing international models: MPI-ESM1-2-HR from Germany's Max Planck Institute for Meteorology[46] and HadGEM3-GC31-LL from the United Kingdom's Met Office Hadley Centre[47]. We focused on three SSP scenarios: SSP1-2.6 (best case), SSP2-4.5 (moderate) and SSP5-8.5 (worst case). Using the Xarray library in Python[68], we read the .nc files into a DataArray with the precipitation and near-surface air temperature data for 2025 and 2050. Oceanic grid points (NaNs) were replaced with zero since we only aim to calculate the projected changes for land where people live. We computed annual total precipitation and mean temperature for each grid cell. These metrics were then used to calculate the De Martonne Aridity Index for both years. We estimated changes in antibiotic resistance by multiplying the projected change in aridity index (2025–2050) by a factor of −0.28, based on the linear relationship in Fig. 3e. Using Python's Cartopy library[69], we visualized projected resistance changes on global PlateCarree maps with colour gradients from dark blue (low) to dark red (high resistance). We constructed an ensemble by stacking projections from all three models, calculating the ensemble mean for each SSP scenario. Projected changes were shown under SSP2-4.5 (moderate case, Extended Data Fig. 9a), SSP1-2.6 (best-case, Extended Data Fig. 9b) and SSP5-8.5 (worst-case, Extended Data Fig. 9c).

Statistics

Statistical analyses, including *t*-tests, Wilcoxon tests and Cohen's *d* effect size[70] calculations, were conducted in R[71] (version 4.4.2). We use one-sided *t*-test to determine the statistical significance of increasing relative abundance of genes and decreasing relative fitness of isolates under drought compared with the control. We use paired Wilcoxon test to determine the statistical significance of increasing relative frequency of antibiotic bacteria under drought compared with control across all sites and all compounds. All *t*-values, degree of freedom, *P* values and number of samples used for each *t*-test are provided in Supplementary Table 1.

Reporting summary

Further information on research design is available in the Nature Portfolio Reporting Summary linked to this article.

Data availability

All data are available within in the article and its Supplementary Information. The following accession numbers allow access to the metagenomic raw data we used from previous studies: cropland metagenomes PRJNA435634, grassland metagenomes PRJNA859194, forest metagenomes PRJEB22281, wetland metagenomes NMDC20147401. Source data are provided with this paper.

References

1. Davies, J. & Davies, D. Origins and evolution of antibiotic resistance. *Microbiol. Mol. Biol. Rev.* **74**, 417–433 (2010).
2. O'Neill, J. Tackling drug-resistant infections globally: final report and recommendations. *CABI Digital Library* https://www.cabidigitallibrary.org/doi/full/10.5555/20173071720 (2016).
3. Lewis, K. The science of antibiotic discovery. *Cell* **181**, 29–45 (2020).
4. Santos-Júnior, C. D. et al. Discovery of antimicrobial peptides in the global microbiome with machine learning. *Cell* **187**, 3761–3778 (2024).
5. Hover, B. M. et al. Culture-independent discovery of the malacidins as calcium-dependent antibiotics with activity against multidrug-resistant Gram-positive pathogens. *Nat. Microbiol.* **3**, 415–422 (2018).
6. Lewis, K. Platforms for antibiotic discovery. *Nat. Rev. Drug Discov.* **12**, 371–387 (2013).
7. Blair, J. M. A., Webber, M. A., Baylay, A. J., Ogbolu, D. O. & Piddock, L. J. V. Molecular mechanisms of antibiotic resistance. *Nat. Rev. Microbiol.* **13**, 42–51 (2014).
8. Allen, H. K. et al. Call of the wild: antibiotic resistance genes in natural environments. *Nat. Rev. Microbiol.* **8**, 251–259 (2010).
9. Wright, G. D. The antibiotic resistome: the nexus of chemical and genetic diversity. *Nat. Rev. Microbiol.* **5**, 175–186 (2007).
10. Perry, E. K., Meirelles, L. A. & Newman, D. K. From the soil to the clinic: the impact of microbial secondary metabolites on antibiotic tolerance and resistance. *Nat. Rev. Microbiol.* **20**, 129–142 (2021).
11. Ault, T. R. On the essentials of drought in a changing climate. *Science* **368**, 256–260 (2020).
12. Mavrodi, D. V. et al. Accumulation of the antibiotic phenazine-1-carboxylic acid in the rhizosphere of dryland cereals. *Appl. Environ. Microbiol.* **78**, 804–812 (2012).
13. Mavrodi, D. V. et al. Long-term irrigation affects the dynamics and activity of the wheat rhizosphere microbiome. *Front. Plant Sci.* **9**, 342036 (2018).
14. Charlop-Powers, Z., Owen, J. G., Reddy, B. V. B., Ternei, M. A. & Brady, S. F. Chemical-biogeographic survey of secondary metabolism in soil. *Proc. Natl Acad. Sci. USA* **111**, 3757–3762 (2014).
15. Bouskill, N. J. et al. Belowground response to drought in a tropical forest soil. II. Change in microbial function impacts carbon composition. *Front. Microbiol.* **7**, 183812 (2016).
16. Xu, L. et al. Genome-resolved metagenomics reveals role of iron metabolism in drought-induced rhizosphere microbiome dynamics. *Nat. Commun.* **12**, 3209 (2021).
17. Santos-Medellín, C., Blazewicz, S. J., Pett-Ridge, J., Firestone, M. K. & Emerson, J. B. Viral but not bacterial community successional patterns reflect extreme turnover shortly after rewetting dry soils. *Nat. Ecol. Evol.* **7**, 1809–1822 (2023).
18. Hartmann, M. et al. Long-term mitigation of drought changes the functional potential and life-strategies of the forest soil microbiome involved in organic matter decomposition. *Front. Microbiol.* **14**, 1267270 (2023).
19. Long, Y. et al. Metagenomic analysis revealing the impact of water contents on the composition of soil microbial communities and the distribution of major ecological functional genes in Poyang Lake wetland soil. *Microorganisms* **12**, 2569 (2024).
20. Medema, M. H. et al. Minimum information about a biosynthetic gene cluster. *Nat. Chem. Biol.* **11**, 625–631 (2015).
21. Parks, D. H. et al. A standardized bacterial taxonomy based on genome phylogeny substantially revises the tree of life. *Nat. Biotechnol.* **36**, 996–1004 (2018).
22. Xu, L. et al. Drought delays development of the sorghum root microbiome and enriches for monoderm bacteria. *Proc. Natl Acad. Sci. USA* **115**, E4284–E4293 (2018).
23. Fitzpatrick, C. R. et al. Assembly and ecological function of the root microbiome across angiosperm plant species. *Proc. Natl Acad. Sci. USA* **115**, E1157–E1165 (2018).
24. Giacalone, D., Schutt, E. & McRose, D. L. The phospho-ferrozine assay: a tool to study bacterial redox-active metabolites produced at the plant root. *Appl. Environ. Microbiol.* **91**, e02194–24 (2025).
25. Honeker, L. K. et al. Drought re-routes soil microbial carbon metabolism towards emission of volatile metabolites in an artificial tropical rainforest. *Nat. Microbiol.* **8**, 1480–1494 (2023).
26. Perry, E. K. & Newman, D. K. Prevalence and correlates of phenazine resistance in culturable bacteria from a dryland wheat field. *Appl. Environ. Microbiol.* **88**, e0232021 (2022).

27. Dar, D., Thomashow, L. S., Weller, D. M. & Newman, D. K. Global landscape of phenazine biosynthesis and biodegradation reveals species-specific colonization patterns in agricultural soils and crop microbiomes. *eLife* **9**, e59726 (2020).
28. Meirelles, L. A. & Newman, D. K. Phenazines and toxoflavin act as interspecies modulators of resilience to diverse antibiotics. *Mol. Microbiol.* **117**, 1384–1404 (2022).
29. Meirelles, L. A., Perry, E. K., Bergkessel, M. & Newman, D. K. Bacterial defenses against a natural antibiotic promote collateral resilience to clinical antibiotics. *PLoS Biol.* **19**, e3001093 (2021).
30. Russell, A. B., Peterson, S. B. & Mougous, J. D. Type VI secretion system effectors: poisons with a purpose. *Nat. Rev. Microbiol.* **12**, 137–148 (2014).
31. Tecon, R., Ebrahimi, A., Kleyer, H., Levi, S. E. & Or, D. Cell-to-cell bacterial interactions promoted by drier conditions on soil surfaces. *Proc. Natl Acad. Sci. USA* **115**, 9791–9796 (2018).
32. Zheng, D. et al. Metagenomics highlights the impact of climate and human activities on antibiotic resistance genes in China's estuaries. *Environ. Pollut.* **301**, 119015 (2022).
33. Beaman, B. L. & Beaman, L. Nocardia species: host–parasite relationships. *Clin. Microbiol. Rev.* **7**, 213–264 (1994).
34. Kirby, R. et al. Draft genome sequence of the human pathogen streptomyces somaliensis, a significant cause of actinomycetoma. *J. Bacteriol.* **194**, 3544–3545 (2012).
35. Smith, I. Mycobacterium tuberculosis pathogenesis and molecular determinants of virulence. *Clin. Microbiol. Rev.* **16**, 463–496 (2003).
36. Scollard, D. M. et al. The continuing challenges of leprosy. *Clin. Microbiol. Rev.* **19**, 338–381 (2006).
37. Forsberg, K. J. et al. The shared antibiotic resistome of soil bacteria and human pathogens. *Science* **337**, 1107–1111 (2012).
38. Jiang, X. et al. Dissemination of antibiotic resistance genes from antibiotic producers to pathogens. *Nat. Commun.* **8**, 15784 (2017).
39. Mahmud, B. et al. Longitudinal dynamics of farmer and livestock nasal and faecal microbiomes and resistomes. *Nat. Microbiol.* **9**, 1007–1020 (2024).
40. Mhuireach, G., Van Den Wymelenberg, K. G. & Langellotto, G. A. Garden soil bacteria transiently colonize gardeners' skin after direct soil contact. *Urban Agric. Region. Food Syst.* **8**, e20035 (2023).
41. Hartmann, E. M. et al. Antimicrobial chemicals are associated with elevated antibiotic resistance genes in the indoor dust microbiome. *Environ. Sci. Technol.* **50**, 9807–9815 (2016).
42. Zhou, Z. et al. Association between particulate matter (PM)2·5 air pollution and clinical antibiotic resistance: a global analysis. *Lancet Planet. Health* **7**, e649–e659 (2023).
43. De Martonne, E. Une nouvelle function climatologique: L'indice d'aridite. *Meteorologie* **2**, 449–459 (1926).
44. O'Neill, B. C. et al. The roads ahead: narratives for shared socioeconomic pathways describing world futures in the 21st century. *Global Environ. Change* **42**, 169–180 (2017).
45. Kelley, M. et al. GISS-E2.1: configurations and climatology. *J. Adv. Model. Earth Syst.* **12**, e2019MS002025 (2020).
46. Gutjahr, O. et al. Max Planck Institute Earth System Model (MPI-ESM1.2) for the High-Resolution Model Intercomparison Project (HighResMIP). *Geosci. Model Dev.* **12**, 3241–3281 (2019).
47. Andrews, M. B. et al. Historical simulations With HadGEM3-GC3.1 for CMIP6. *J. Adv. Model. Earth Syst.* **12**, e2019MS001995 (2020).
48. Li, X. J. et al. Uncertainties in global permafrost area extent estimates from different methods. *Adv. Clim. Chang. Res.* **16**, 312–323 (2025).
49. Falghoush, A., Beyenal, H., Besser, T. E., Omsland, A. & Call, D. R. Osmotic compounds enhance antibiotic efficacy against *Acinetobacter baumannii* biofilm communities. *Appl. Environ. Microbiol.* **83**, e01297–17 (2017).
50. Barraud, N., Buson, A., Jarolimek, W. & Rice, S. A. Mannitol enhances antibiotic sensitivity of persister bacteria in *Pseudomonas aeruginosa* biofilms. *PLoS ONE* **8**, e84220 (2013).
51. Al-Nabulsi, A. A. et al. Effects of osmotic pressure, acid, or cold stresses on antibiotic susceptibility of Listeria monocytogenes. *Food Microbiol.* **46**, 154–160 (2015).
52. Hood, M. I., Jacobs, A. C., Sayood, K., Dunman, P. M. & Skaar, E. P. *Acinetobacter baumannii* increases tolerance to antibiotics in response to monovalent cations. *Antimicrob. Agents Chemother.* **54**, 1029–1041 (2010).
53. Windham, I. H. & Merrell, D. S. Interplay between amoxicillin resistance and osmotic stress in *Helicobacter pylori*. *J. Bacteriol.* **204**, e0004522 (2022).
54. Xu, X. et al. Adsorption/desorption and degradation of doxycycline in three agricultural soils. *Ecotoxicol. Environ. Saf.* **224**, 112675 (2021).
55. Huang, S. et al. Dry-to-wet fluctuation of moisture contents enhanced the mineralization of chloramphenicol antibiotic. *Water Res.* **240**, 120103 (2023).
56. Hernando-Amado, S., Coque, T. M., Baquero, F. & Martínez, J. L. Defining and combating antibiotic resistance from One Health and Global Health perspectives. *Nat. Microbiol.* **4**, 1432–1442 (2019).
57. Zambrano, M. M. Interplay between antimicrobial resistance and global environmental change. *Annu. Rev. Genet.* **57**, 275–296 (2023).
58. Alcock, B. P. et al. CARD 2023: expanded curation, support for machine learning, and resistome prediction at the Comprehensive Antibiotic Resistance Database. *Nucleic Acids Res.* **51**, D690–D699 (2023).
59. Chen, S., Zhou, Y., Chen, Y. & Gu, J. fastp: an ultra-fast all-in-one FASTQ preprocessor. *Bioinformatics* **34**, i884–i890 (2018).
60. Buchfink, B., Xie, C. & Huson, D. H. Fast and sensitive protein alignment using DIAMOND. *Nat. Methods* **12**, 59–60 (2014).
61. Zhang, J. et al. SecReT6 update: a comprehensive resource of bacterial type VI secretion systems. *Sci. China Life Sci.* **66**, 626–634 (2022).
62. Steinegger, M. & Söding, J. MMseqs2 enables sensitive protein sequence searching for the analysis of massive data sets. *Nat. Biotechnol.* **35**, 1026–1028 (2017).
63. visNetwork, an R package for interactive network visualization. *GitHub* http://datastorm-open.github.io/visNetwork/ (2022).
64. GNI per capita, Atlas method (current US$). *World Bank Group* http://data.worldbank.org/indicator/NY.GNP.PCAP.CD (2025).
65. Thrasher, B. et al. NASA global daily downscaled projections. *CMIP6. Sci. Data* **9**, 262 (2022).
66. Thrasher B., Wang W., Michaelis A. & Nemani R. NEX-GDDP-CMIP6. *NASA Center for Climate Simulations* https://doi.org/10.7917/OFSG3345 (2021).
67. Eyring, V. et al. Overview of the Coupled Model Intercomparison Project Phase 6 (CMIP6) experimental design and organization. *Geosci. Model Dev.* **9**, 1937–1958 (2016).
68. Hoyer, S. & Hamman, J. J. xarray: N-D labeled arrays and datasets in Python. *J. Open Res. Softw.* **5**, 10 (2017).
69. Cartopy—a cartographic python library with matplotlib support. *GitHub* http://github.com/SciTools/cartopy (2026).
70. Ben-Shachar, M. S., Lüdecke, D. & Makowski, D. Effectsize: estimation of effect size indices and standardized parameters. *J. Open Source Softw.* **5**, 2815 (2020).
71. R Core Team. R: A Language and Environment for Statistical Computing (R Foundation for Statistical Computing, 2017).
72. Cohen, J. *Statistical Power Analysis for the Behavioral Sciences* 2nd edn. https://doi.org/10.4324/9780203771587 (Routledge, 1988).

Acknowledgements
We thank O. Cordero, D. McRose, J. Fink, P. Bravo, A. Flamholz and all members of the Newman lab for useful feedback. We thank H. Chen and Z. Zhou at Zhejiang University for their generous sharing of the global hospital antibiotic resistance dataset. We thank Z. Long and Y. Long at Jiangxi Normal University for help in accessing metagenomic raw data. X.S. thanks Y. Wang and K. Zhao for helpful discussions on soil ecology. This research was supported by the Doren Family Foundation and the Resnick Sustainability Institute. X.S. received a Nemko Postdoctoral Fellowship from the BBE Division at Caltech; H.J. was supported by a Helen Hay Whitney Postdoctoral Fellowship; R.E.A. was supported by a BBE Divisional Fellowship and an NSF Postdoctoral Research Fellowship (2209379); I.B.T. was supported by an EMBO Postdoctoral Fellowship (ALTF 191-2023); J.V.K. was supported by an NSF Graduate Research Fellowship.

Author contributions
X.S. and D.K.N conceived the idea, developed the project, interpreted the data, and wrote the paper. X.S. performed experiments and all bioinformatic analyses. K.C. analysed GCM data. H.J. contributed to the development of the soil microcosm assay. R.E.A. and J.V.K. assisted in formulating the concept of drought-induced concentration effects. I.B.T. contributed to strain phenotyping and assisted with data interpretation. All authors edited the paper.

Competing interests
The authors declare no competing interests.

Additional information
Extended data is available for this paper at https://doi.org/10.1038/s41564-026-02274-x.

Supplementary information The online version contains supplementary material available at https://doi.org/10.1038/s41564-026-02274-x.

Correspondence and requests for materials should be addressed to Dianne K. Newman.

Peer review information *Nature Microbiology* thanks Arnaud Dechesne, Timothy Ghaly and Alejandra Rodríguez-Verdugo for their contribution to the peer review of this work. Peer reviewer reports are available.

https://doi.org/10.1038/s41564-026-02274-x

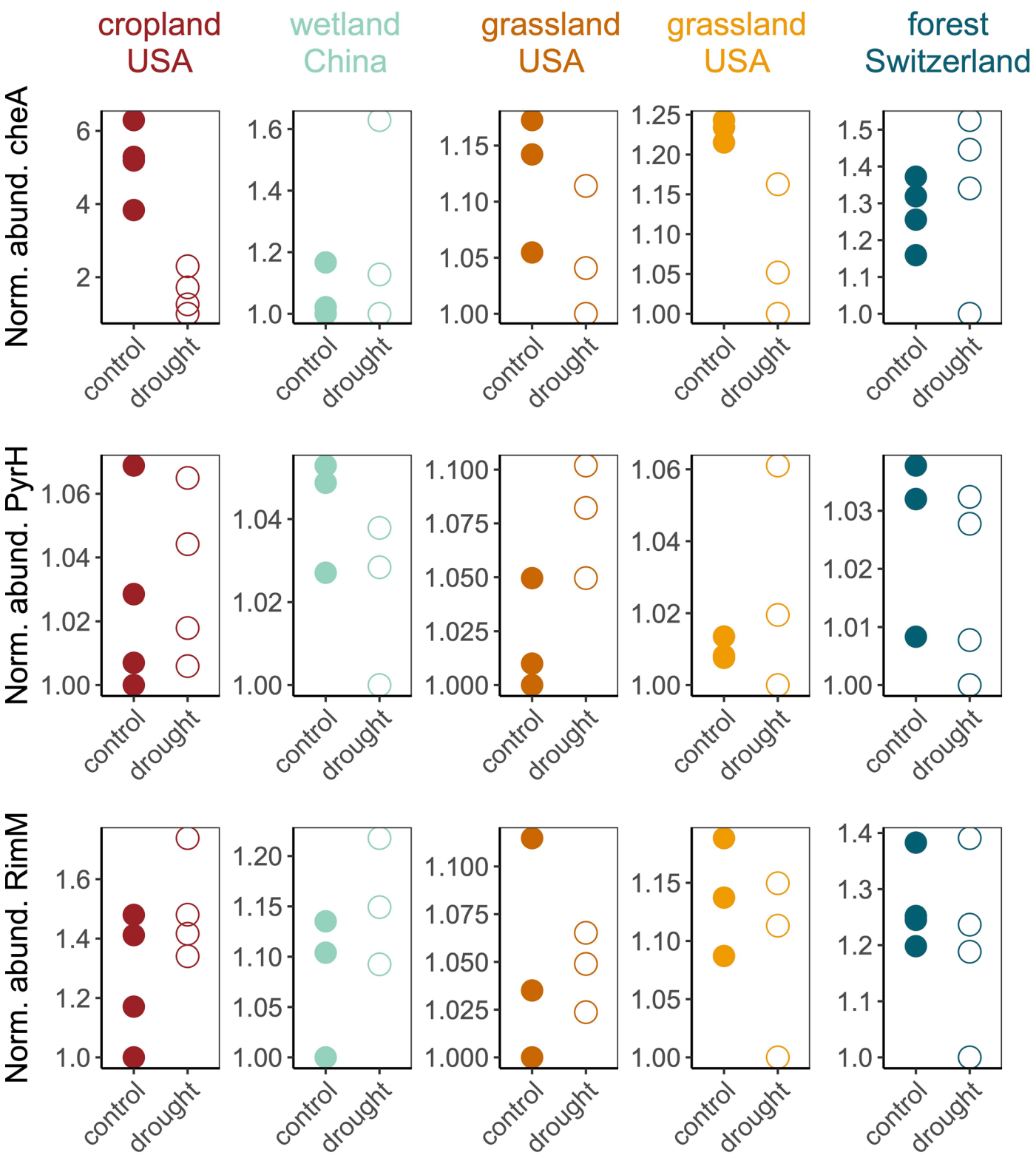

Extended Data Fig. 1 | Normalized relative abundance of control genes under drought and control. Top panel: Bacterial chemotaxis gene *cheA*; middle panel: UMP kinase *pyrH*; bottom panel: ribosomal maturation protein *RimM*. Closed dots indicate drought and open dots indicate control. P values, degree of freedom and t statistics are reported in Table S1.

https://doi.org/10.1038/s41564-026-02274-x

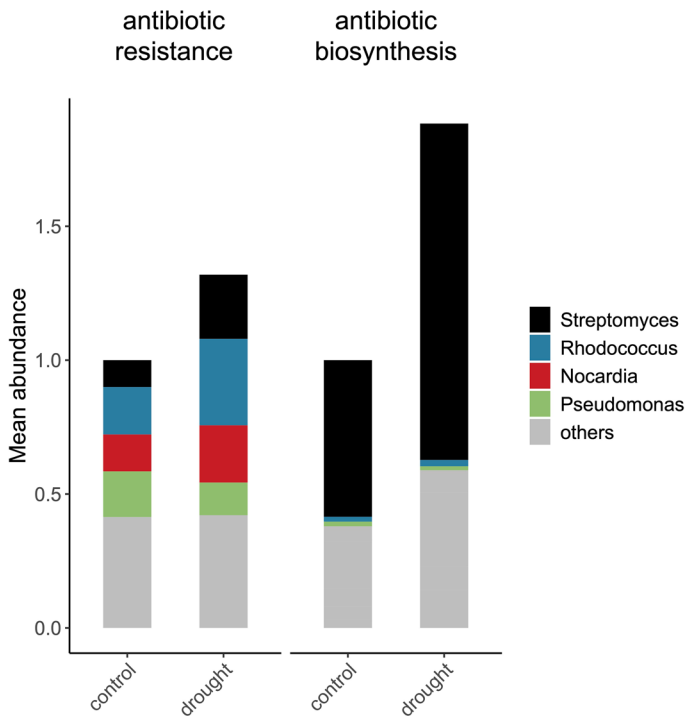

Extended Data Fig. 2 | Taxonomic composition of antibiotic resistance genes and antibiotic biosynthesis genes. Mean relative abundance is normalized to the minimal values for each group. Taxonomic assignments are based on the best-matching reference genes in the MiBIG database (for antibiotic biosynthesis genes) or the CARD database (for antibiotic resistance genes).

https://doi.org/10.1038/s41564-026-02274-x

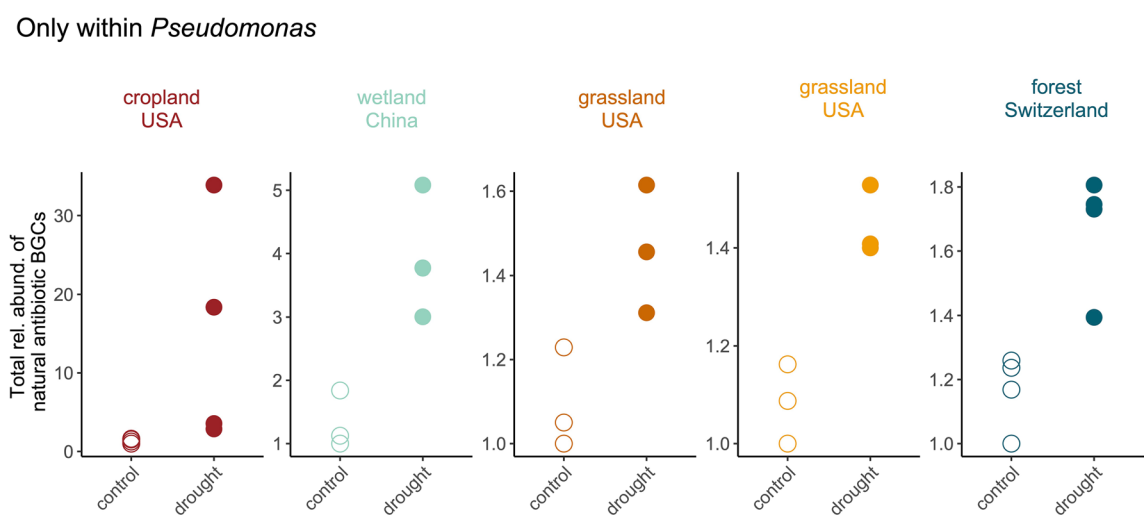

Extended Data Fig. 3 | Abundance of *Pseudomonas*-derived antibiotic BGCs normalized by *Pseudomonas* population abundance. Enrichment of antibiotic resistance biosynthesis genes remains significant within *Pseudomonas*. Closed dots indicate drought while open dots indicate control.

https://doi.org/10.1038/s41564-026-02274-x

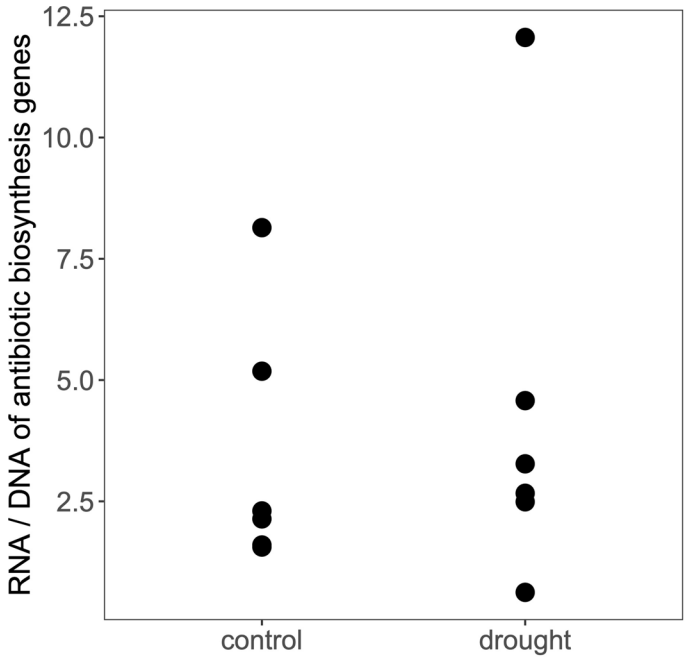

Extended Data Fig. 4 | Relative expression level of natural antibiotic biosynthesis genes under drought and control conditions. Relative expression level is quantified as the ratio of metatranscriptomic reads per kilobase and metagenomic reads per kilobase. There are no significant differences between drought and control ($P = 0.69$). The data was originally from ref. 32.

https://doi.org/10.1038/s41564-026-02274-x

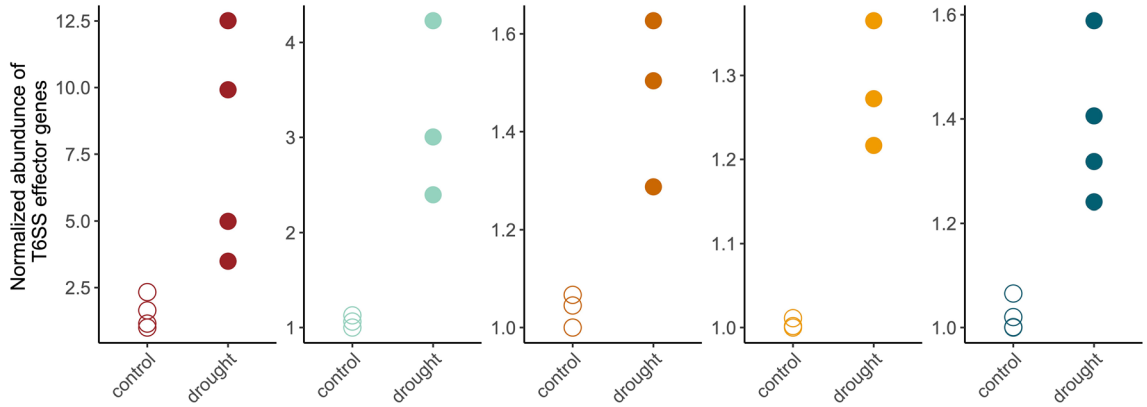

Extended Data Fig. 5 | Significant enrichment of T6SS effector genes within the *Pseudomonas* population. Closed dots indicate drought while open dots indicate control.

https://doi.org/10.1038/s41564-026-02274-x

Extended Data Fig. 6 | Sampling sites of natural soil at Caltech campus. A: 34.1372149 N, 118.1276953 W; B: 34.1367032 N, 118.1268789 W; C: 34.1367229 N, 118.1243942 W.

https://doi.org/10.1038/s41564-026-02274-x

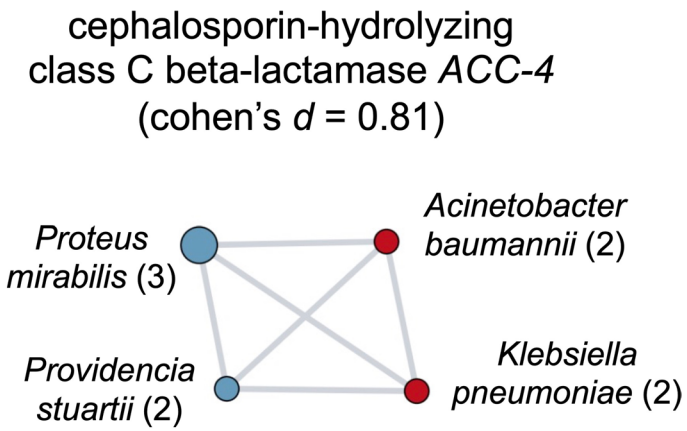

Extended Data Fig. 7 | Recent horizontal gene transfer of drought-enriched antibiotic resistance genes across ESKAPE pathogens. Red nodes indicate ESKAPE pathogens and blue nodes indicate non-ESKAPE pathogens often found in soil. Edges represent 100% sequence identity. Values in brackets indicate the number of genomes harboring 100% identical sequences. Network structure was visualized by R package visNetwork.

https://doi.org/10.1038/s41564-026-02274-x

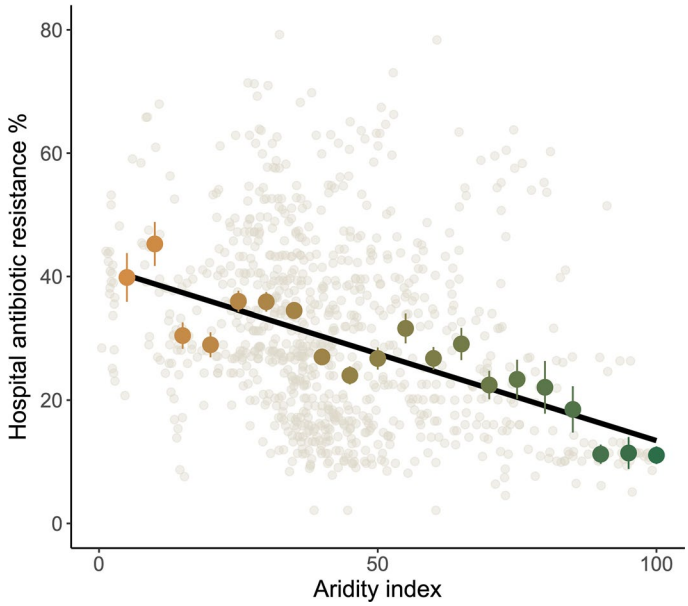

Extended Data Fig. 8 | Correlation between clinical resistance and aridity. The correlation is shown at the level of individual data points (n = 913) prior to averaging shown in Fig. 3e. A significant negative correlation remains when using all individual observations (Pearson's r = − 0.34, $P < 10^{-16}$), indicating that the trend still holds even without aggregating the data. Data are presented as mean values ± standard error.

https://doi.org/10.1038/s41564-026-02274-x

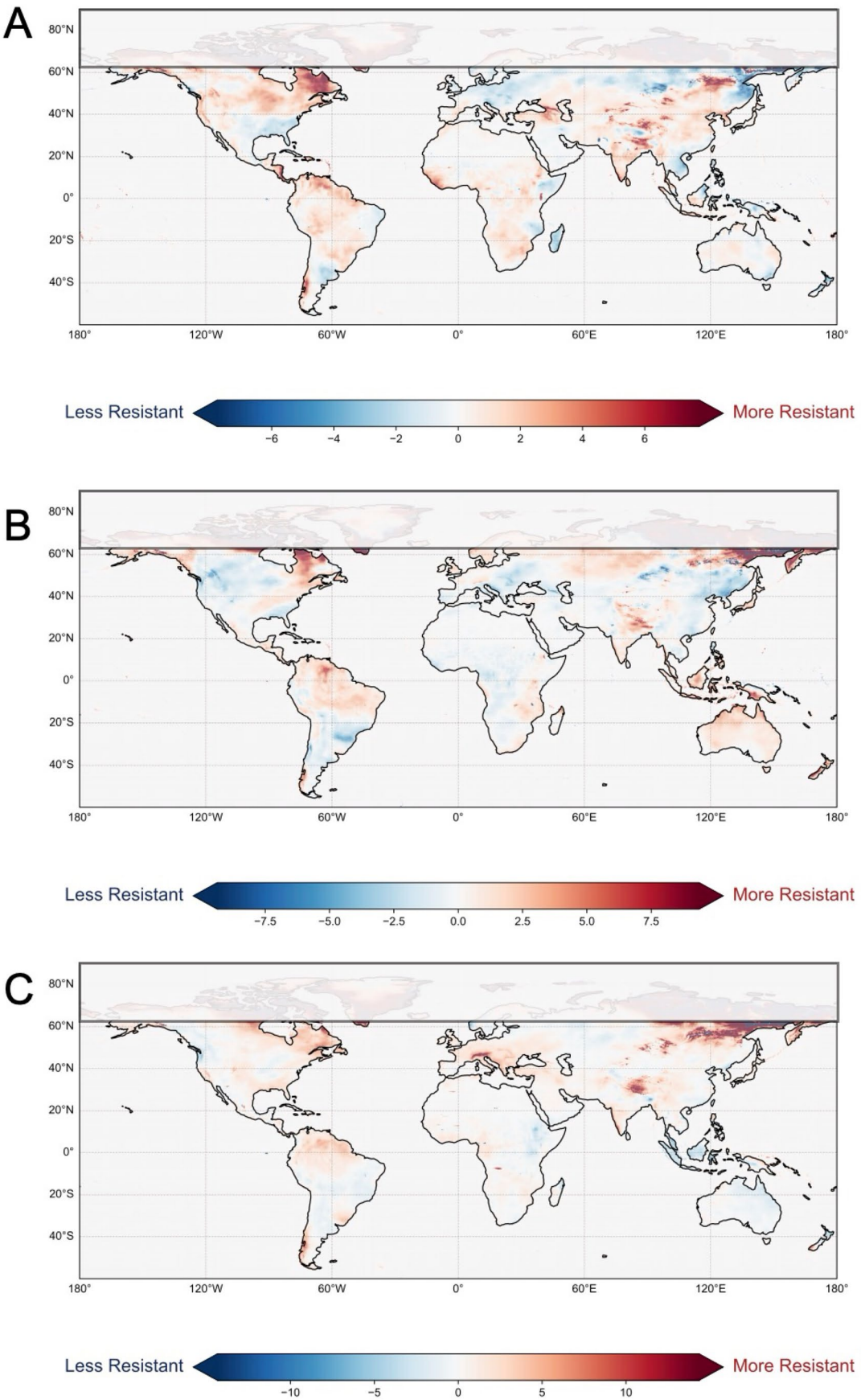

Extended Data Fig. 9 | Projected antibiotic resistance changes. We exclude latitudes greater than 60 °N covered by permafrost[34], under (**A**) SSP2-4.5 scenario, (**B**) SSP1-2.6 scenario and (**C**) SSP5-8.5 scenario.

nature portfolio

Corresponding author(s): Dianne K. Newman
Last updated by author(s): Xiaoyu Shan

Reporting Summary

Nature Portfolio wishes to improve the reproducibility of the work that we publish. This form provides structure for consistency and transparency in reporting. For further information on Nature Portfolio policies, see our Editorial Policies and the Editorial Policy Checklist.

Statistics

For all statistical analyses, confirm that the following items are present in the figure legend, table legend, main text, or Methods section.

n/a	Confirmed	
☐	☒	The exact sample size (*n*) for each experimental group/condition, given as a discrete number and unit of measurement
☐	☒	A statement on whether measurements were taken from distinct samples or whether the same sample was measured repeatedly
☐	☒	The statistical test(s) used AND whether they are one- or two-sided *Only common tests should be described solely by name; describe more complex techniques in the Methods section.*
☐	☒	A description of all covariates tested
☒	☐	A description of any assumptions or corrections, such as tests of normality and adjustment for multiple comparisons
☐	☒	A full description of the statistical parameters including central tendency (e.g. means) or other basic estimates (e.g. regression coefficient) AND variation (e.g. standard deviation) or associated estimates of uncertainty (e.g. confidence intervals)
☐	☒	For null hypothesis testing, the test statistic (e.g. *F*, *t*, *r*) with confidence intervals, effect sizes, degrees of freedom and *P* value noted *Give P values as exact values whenever suitable.*
☒	☐	For Bayesian analysis, information on the choice of priors and Markov chain Monte Carlo settings
☒	☐	For hierarchical and complex designs, identification of the appropriate level for tests and full reporting of outcomes
☐	☒	Estimates of effect sizes (e.g. Cohen's *d*, Pearson's *r*), indicating how they were calculated

Our web collection on statistics for biologists contains articles on many of the points above.

Software and code

Policy information about availability of computer code

Data collection	The following databases were used, as described in the Methods section: MIBiG version 4.0, CARD (release December 2024), SecReT6 (version 3), NEX-GDDP-CMIP6, GISS-E2-1-G, MPI-ESM1-2-HR, HadGEM3-GC31-LL, and hospital data from reference 43 (Zhou et al., 2023)
Data analysis	The following packages were used for data analysis, as described in the Methods section: DIAMOND (version 2.1.8.162), MMseqs2 (version f6c98807d589091c625db68da258d587795acbab), R package visNetwork, Python's Cartopy library version 0.24, R version 4.4.2

For manuscripts utilizing custom algorithms or software that are central to the research but not yet described in published literature, software must be made available to editors and reviewers. We strongly encourage code deposition in a community repository (e.g. GitHub). See the Nature Portfolio guidelines for submitting code & software for further information.

Data

Policy information about availability of data

All manuscripts must include a data availability statement. This statement should provide the following information, where applicable:

- Accession codes, unique identifiers, or web links for publicly available datasets
- A description of any restrictions on data availability
- For clinical datasets or third party data, please ensure that the statement adheres to our policy

All data supporting the findings of this study are available within the paper and its Supplementary Information. Full references to datasets utilized in the study are provided. The following accession numbers allow access to the data we used: Cropland metagenomes PRJNA435634, Grassland metagenomes PRJNA859194

Forest metagenomes PRJEB22281, Wetland metagenomes NMDC20147401

Research involving human participants, their data, or biological material

Policy information about studies with human participants or human data. See also policy information about sex, gender (identity/presentation), and sexual orientation and race, ethnicity and racism.

Reporting on sex and gender	*Use the terms sex (biological attribute) and gender (shaped by social and cultural circumstances) carefully in order to avoid confusing both terms. Indicate if findings apply to only one sex or gender; describe whether sex and gender were considered in study design; whether sex and/or gender was determined based on self-reporting or assigned and methods used.* *Provide in the source data disaggregated sex and gender data, where this information has been collected, and if consent has been obtained for sharing of individual-level data; provide overall numbers in this Reporting Summary. Please state if this information has not been collected.* *Report sex- and gender-based analyses where performed, justify reasons for lack of sex- and gender-based analysis.*
Reporting on race, ethnicity, or other socially relevant groupings	*Please specify the socially constructed or socially relevant categorization variable(s) used in your manuscript and explain why they were used. Please note that such variables should not be used as proxies for other socially constructed/relevant variables (for example, race or ethnicity should not be used as a proxy for socioeconomic status).* *Provide clear definitions of the relevant terms used, how they were provided (by the participants/respondents, the researchers, or third parties), and the method(s) used to classify people into the different categories (e.g. self-report, census or administrative data, social media data, etc.)* *Please provide details about how you controlled for confounding variables in your analyses.*
Population characteristics	*Describe the covariate-relevant population characteristics of the human research participants (e.g. age, genotypic information, past and current diagnosis and treatment categories). If you filled out the behavioural & social sciences study design questions and have nothing to add here, write "See above."*
Recruitment	*Describe how participants were recruited. Outline any potential self-selection bias or other biases that may be present and how these are likely to impact results.*
Ethics oversight	*Identify the organization(s) that approved the study protocol.*

Note that full information on the approval of the study protocol must also be provided in the manuscript.

Field-specific reporting

Please select the one below that is the best fit for your research. If you are not sure, read the appropriate sections before making your selection.

☐ Life sciences ☐ Behavioural & social sciences ☒ Ecological, evolutionary & environmental sciences

For a reference copy of the document with all sections, see nature.com/documents/nr-reporting-summary-flat.pdf

Ecological, evolutionary & environmental sciences study design

All studies must disclose on these points even when the disclosure is negative.

Study description	Drought vs. control was the only variable for the study design.
Research sample	Soil samples from various locations and soil types, including cropland, grassland, forest and wetland.
Sampling strategy	At least three replicate samples were included to facilitate comparative analysis with statistical significance/
Data collection	All metagenomic data was collected from publicly available databases. Experimental data was collected via CFU counting in the lab by the leading author.
Timing and spatial scale	Studies with metagenomic sampling spanned various timescales (three days to three months), as reported in the Methods section and in each cited metagenomic study. Experimental studies had drought treatment for three days in the lab to mimic short-term exposure to water-limited conditions.
Data exclusions	No data was excluded.
Reproducibility	For metagenomic samples, at least three replicate samples were included in the analyses. For experimental studies, CFU counting was performed for at least two biological replicates.
Randomization	Not relevant to this study.
Blinding	Not relevant to this study.

Did the study involve field work? ☐ Yes ☒ No

Reporting for specific materials, systems and methods

We require information from authors about some types of materials, experimental systems and methods used in many studies. Here, indicate whether each material, system or method listed is relevant to your study. If you are not sure if a list item applies to your research, read the appropriate section before selecting a response.

Materials & experimental systems

n/a	Involved in the study
☒	☐ Antibodies
☒	☐ Eukaryotic cell lines
☒	☐ Palaeontology and archaeology
☒	☐ Animals and other organisms
☒	☐ Clinical data
☒	☐ Dual use research of concern
☒	☐ Plants

Methods

n/a	Involved in the study
☒	☐ ChIP-seq
☒	☐ Flow cytometry
☒	☐ MRI-based neuroimaging

Plants

Seed stocks

Report on the source of all seed stocks or other plant material used. If applicable, state the seed stock centre and catalogue number. If plant specimens were collected from the field, describe the collection location, date and sampling procedures.

Novel plant genotypes

Describe the methods by which all novel plant genotypes were produced. This includes those generated by transgenic approaches, gene editing, chemical/radiation-based mutagenesis and hybridization. For transgenic lines, describe the transformation method, the number of independent lines analyzed and the generation upon which experiments were performed. For gene-edited lines, describe the editor used, the endogenous sequence targeted for editing, the targeting guide RNA sequence (if applicable) and how the editor was applied.

Authentication

Describe any authentication procedures for each seed stock used or novel genotype generated. Describe any experiments used to assess the effect of a mutation and, where applicable, how potential secondary effects (e.g. second site T-DNA insertions, mosiacism, off-target gene editing) were examined.